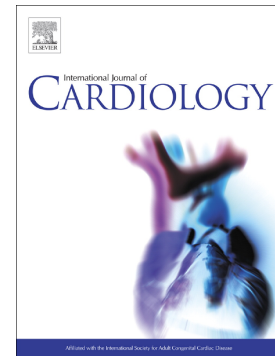


Diphosphonate single-photon emission computed tomography in cardiac transthyretin amyloidosis

Chrysanthos Grigoratos, Alberto Aimò, Claudio Rapezzi, Dario Genovesi, Andrea Barison, Giovanni Donato Aquaro, Giuseppe Vergaro, Angela Pucci, Claudio Passino, Paolo Marzullo, Alessia Gimelli, Michele Emdin



PII: S0167-5273(19)35840-1

DOI: <https://doi.org/10.1016/j.ijcard.2020.02.030>

Reference: IJCA 28360

To appear in: *International Journal of Cardiology*

Received date: 24 November 2019

Revised date: 26 January 2020

Accepted date: 10 February 2020

Please cite this article as: C. Grigoratos, A. Aimò, C. Rapezzi, et al., Diphosphonate single-photon emission computed tomography in cardiac transthyretin amyloidosis, *International Journal of Cardiology*(2020), <https://doi.org/10.1016/j.ijcard.2020.02.030>

This is a PDF file of an article that has undergone enhancements after acceptance, such as the addition of a cover page and metadata, and formatting for readability, but it is not yet the definitive version of record. This version will undergo additional copyediting, typesetting and review before it is published in its final form, but we are providing this version to give early visibility of the article. Please note that, during the production process, errors may be discovered which could affect the content, and all legal disclaimers that apply to the journal pertain.

Diphosphonate Single-Photon Emission Computed Tomography in Cardiac Transthyretin Amyloidosis

Chrysanthos Grigoratos, MD^{a,b*}, Alberto Aimò, MD^{b*}, Claudio Rapezzi, MD^c, Dario Genovesi, MD^a, Andrea Barison, MD, PhD^{a,b}, Giovanni Donato Aquaro, MD^a, Giuseppe Vergaro, MD, PhD^{a,b}, Angela Pucci, MD, PhD^d, Claudio Passino, MD, PhD^{a,b}, Paolo Marzullo, MD^a, Alessia Gimelli, MD^a, Michele Emdin, MD, PhD^{a,b},

* Chrysanthos Grigoratos and Alberto Aimò equally contributed

a. Fondazione Toscana Gabriele Monasterio, Pisa, Italy; b. Institute of Life Sciences, Scuola Superiore Sant'Anna, Pisa, Italy; c. Department of Experimental, Diagnostic, and Specialty Medicine, University of Bologna, Bologna, Italy; d. Histopathology Department, University Hospital of Pisa, Italy.

Short title: SPECT in cardiac amyloidosis.

Word count: 2461 (text)

Disclosures: none

Address for correspondence:

Chrysanthos Grigoratos, MD

Fondazione Toscana Gabriele Monasterio, Pisa, Italy

Via Moruzzi 1. 56124, Pisa, Italy

Phone +39 0503152824

Fax +39 0503152109

Email: cgrigoratos@ftgm.it

Abstract

Background: Planar diphosphonate scintigraphy is an established diagnostic tool for amyloid transthyretin (ATTR) cardiomyopathy. Characterization of the amyloid burden up to the segmental level by single photon emission computed tomography (SPECT) has not been evaluated so far.

Methods: Data from consecutive patients undergoing cardiac ^{99m}Tc -hydroxymethylene diphosphonate (^{99m}Tc -HMDP) SPECT and diagnosed with ATTR cardiomyopathy at a tertiary referral center from June 2016 to April 2019 were collected.

Results: Thirty-eight patients were included (median age 81 years, 79% men, 92% with wild-type ATTR). In patients with Perugini score 1, the most intense diphosphonate regional uptake was found in septal segments, particularly in infero-septal segments. Among patients scoring 2, the amyloid burden in the septum became more significant, and extended to inferior and apical segments. Finally, patients scoring 3 displayed an intense and widespread tracer uptake. All patients with Perugini score 1 had LGE in at least one antero-septal, one infero-septal, and one infero-lateral segment. All patients with score 2 displayed LGE in infero-septal, inferior, and infero-lateral segments. LGE became extensive in patients scoring 3, with all patients having at least one LGE-positive segment in each region.

Conclusions: When assimilating different Perugini grades to evolutive stages of the disease, amyloid deposition seem to progress from the septum to the inferior wall and then to the other regions and from the basis to the apex. The potential of segmental analysis might be particularly relevant in patients with very limited cardiac uptake at planar scintigraphy (Perugini score 1).

Word count: 243 (abstract)

Keywords

Transthyretin amyloidosis, diphosphonate, SPECT, cardiac magnetic resonance

Abbreviation list

ATTR, amyloid transthyretin

CMR, cardiac magnetic resonance

CZT, Cadmium Zinc Telluride

HF, heart failure

LV, left ventricular

SPECT, single photon emission computed tomography

^{99m}Tc -HMDP, ^{99m}Tc -hydroxymethylene diphosphonate

Introduction

Transthyretin (TTR) is a tetrameric protein synthesized mostly by the liver. As a result of gene mutations or as an ageing-related phenomenon, TTR molecules may misfold and deposit in the heart and in other organs as amyloid fibrils [1]. Cardiac involvement in amyloid TTR (ATTR) amyloidosis typically manifests as left ventricular (LV) pseudohypertrophy and/or heart failure (HF) with preserved ejection fraction. ATTR is increasingly recognized as an underdiagnosed condition [2], as well as a crucial determinant of morbidity and mortality.

Cardiac ATTR can be diagnosed through the demonstration of TTR amyloid deposits on endomyocardial biopsy or following a non-invasive algorithm that includes cardiac magnetic resonance (CMR) and diphosphonate scintigraphy [3]. Planar scintigraphy with the use of ^{99m}Tc -labelled diphosphonate tracers has proven a valuable tool to detect the presence of myocardial TTR amyloid deposits [4], and to perform a qualitative assessment of the amyloid burden through the Perugini scoring system [5]. Compared to planar imaging, single-photon emission computed tomography (SPECT) examination allows a 3-dimensional assessment of myocardial tracer uptake. Techniques for SPECT imaging are now commonly available, given their role in the diagnostic work-up of coronary artery disease [6], and has been further refined thanks to the introduction of the Cadmium Zinc Telluride (CZT) technique, which allows better spatial resolution and sensitivity [7].

In the present study we evaluated the potential of CZT SPECT imaging for detecting myocardial infiltration in ATTR-related cardiac disease, also in comparison with CMR.

Methods

Patient population

Data from consecutive patients evaluated at a tertiary referral center in Italy from June 2016 to April 2019, undergoing both cardiac diphosphonate scintigraphy with SPECT acquisitions and

CMR as part of their diagnostic workup, and ultimately diagnosed with ATTR cardiomyopathy were retrospectively collected. Cardiac ATTR amyloidosis was diagnosed according to the algorithm by Gillmore et al., whereby histological confirmation and typing of amyloid is not required when patients score 2-3 on the Perugini scale and have no monoclonal protein [3]. Patients provided written informed consent for each examination, as well as data collection and analysis.

Echocardiographic examination

Standard, 2-dimensional transthoracic images were obtained using a Philips IE33 Ultrasound machine, with X5-1 transducer (Philips Medical Systems, Palo Alto, California, USA). Standard techniques were used to assess wall thickness, chamber volumes, and indices of systolic and diastolic function, and volumes were measured using the biplane method of disks (modified Simpson's method). The reading protocol was standardized and consistent across years.

Cardiac magnetic resonance

All patients without contraindications were examined by a 1.5-T unit (CVi, GE-Healthcare, Milwaukee, USA) using a dedicated cardiac software, 8-channel phased-array surface receiver coil and vectorcardiogram triggering. Ventricular function was assessed by short-axis steady-state free precession cine imaging (field-of-view: 380–400 mm, repetition/echo time: 3.2/1.6 ms, flip angle: 60°, matrix: 224 × 192, phases: 30, thickness: 8 mm, no gap). LGE imaging was performed 10 to 20 min after gadolinium administration using a segmented T1-weighted gradient-echo inversion-recovery pulse sequence (field-of-view: 380–400 mm, slice thickness: 8 mm, repetition/echo time: 4.6/1.3 ms, flip angle: 208, matrix: 256×192). The inversion time (IT) was individually adapted to suppress the signal of normal remote myocardium (220-300 ms); in all cases, a midventricular short-axis TI-scout sequence was used to choose the appropriate inversion time and to check the presence of paradoxical blood/myocardium inversion times. When no normal myocardium was found, the IT was chosen using conventional values to suppress normal myocardium and make

enhanced myocardium look bright; in such cases, the whole myocardium was nulled before the blood pool in the IT scout sequence.

LV and RV volumes, wall thickness, mass and global function were determined from the stack of short-axis cine by 2 experienced CMR readers (C.G., A.B.), blinded to SPECT results. The presence and pattern of LGE were visually determined on post-contrast short-axis and long-axis images by the same 2 operators; in cases of disagreement, a third operator (G.D.A.) was consulted.

Scintigraphy examination

^{99m}Tc -hydroxymethylene diphosphonate (^{99m}Tc -HMDP) was prepared from a commercial kit (OSTEOCIS). Each patient received intravenous 700-740 MBq of ^{99m}Tc -HMDP, and a whole-body scan (anterior and posterior projections) was performed 150 min later, in a 256*1024 matrix (E.Cam; Siemens Medical Solution; Hoffman Estates, IL, USA). All patients then underwent a CZT tomographic acquisition using a dedicated cardiac camera (Discovery NM 530c; GE Healthcare; Haifa, Israel).

Planar images were acquired with a standard SPECT camera using low-energy, high-resolution collimators and an appropriate scan speed to reach over 2×10^6 counts. Cardiac uptake was graded according to the Perugini system as: grade 0, no cardiac uptake; grade 1, cardiac uptake present but less intense than the bone signal; grade 2, cardiac uptake with intensity similar or greater than bone signal; grade 3, cardiac uptake with much attenuated or absent bone signal [8]. All patients then underwent a CZT acquisition, lasting about 6 minutes. The system design enabled a high-quality imaging of a 3-dimensional volume where the patient's heart was positioned. CZT images were reconstructed on a standard workstation (Xeleris II; GE Healthcare) using a previously validated dedicated iterative algorithm with 50 iterations. A Butterworth post-processing filter (frequency 0.37, order 7) was applied to the reconstructed slices. Images were reconstructed without correction for scatter or attenuation.

Quantitative analysis of tracer uptake was performed using normalized polar maps and a 17-segment LV model. Segmental ^{99m}Tc -HMDP tracer uptake was calculated as percentage of the peak tracer uptake, and classified using the following scale: 0=normal (<10% uptake), 1=mild increase of tracer uptake (10-29%), 2=moderate increase (30-49%), 3=severe increase (50-69%), 4=very severe increase (70-100%). The following LV regions were also considered: anterior (segments 1, 7), antero-septal (2, 8), infero-septal (3, 9), inferior (4, 10), infero-lateral (5, 11), antero-lateral (6, 12), apical (13-17). For each patient, the average tracer uptake in segments composing each region was calculated.

Statistical analysis

Statistical analysis was performed using IBM SPSS Statistics (version 22, 2013). Normal distribution was assessed through the Kolmogorov-Smirnov test; as all variables had non-normal distribution, they were expressed as median and interquartile interval. Differences between groups were tested through the Mann-Whitney U test. Categorical variables were compared by the Chi-square test with Yates correction. p values <0.05 were considered statistically significant.

Results

Study population, echocardiographic and cardiac magnetic resonance findings

The main characteristics of study population (n=38) are reported in **Table 1**. Mean age was 81 years, and 30 patients (79%) were men. The vast majority (n=35, 92%) was diagnosed with wild-type ATTR, and 3 (8%) with variant ATTR. Interventricular septum and posterior wall thickness, relative wall thickness (RWT), and E/e' ratio values were all increased. Among patients undergoing CMR scan (n=35, 92%), median LV ejection fraction was 55% (47-65), and LV mass index was increased (125 g/m^2 [99-151]). Three patients (8%) scored 1 on the Perugini scale; the diagnosis was made following demonstration of ATTR amyloid on endomyocardial biopsy (2 patients), or periumbilical fat biopsy (1 patient). Twenty patients (53%) scored 2, and 15 (40%) scored 3. In

parallel with increasing Perugini score values, a progressive increase in wall thickness and RWT, and a trend towards increased LV mass index were noted (**Table 1**).

Perugini grades vs. SPECT: percent diphosphonate uptake

SPECT imaging was deemed of high quality in all cases. In patients scoring 1 on the Perugini scale (n=3), the most intense diphosphonate uptake was found in septal segments, particularly in infero-septal segments (3 and 9). Antero-septal segments (2 and 8) and the apical septal segment (14) followed, while the lowest uptake was observed in some apical segments, namely apical inferior (15), lateral (16), and apex (17).

Among patients scoring 2 (n=20), the amyloid burden in the septal region became more significant, and extended to the inferior region (segments 4 and 10), and some apical segments (14 and 15). Finally, a diffuse and intense uptake was found in patients scoring 3 (n=15), involving also the anterior, lateral, and apical regions (**Figures 1 and 2, Supplemental Figure 1**). The basal-to-apical ratio of diphosphonate uptake was lower than in patients scoring 1 or 2, reflecting greater amyloid accumulation in the apical region (**Figure 3**).

Perugini grades and SPECT vs. LGE analysis

All patients scoring 1 on the Perugini scale had LGE in at least one antero-septal segment (2, 8), one infero-septal segment (3, 9), and one infero-lateral segment (5,11). Conversely, LGE was found in at least 1 apical segment (13-17) in a single patient. Among patients scoring 2, all displayed LGE in the infero-septal, inferior, and infero-lateral regions; among apical segments, the apical septal (14) and apical inferior (15) were those most often showing LGE. When progressing to Perugini grade 3, LGE became extensive, with all patients displaying at least one LGE-positive segment in each region (**Supplemental Figure 2**). In the whole population, patients with LGE in a segment or region consistently displayed a more intense ^{99m}Tc -HMDP uptake than those with no LGE (**Supplemental Figure 3**). Finally, a good agreement was found between severe or very severe

^{99m}Tc -HMDP tracer uptake (>50%) and LGE presence at both segmental and regional level (Supplemental Table 1).

Discussion

The present study represents the first dedicated assessment of diphosphonate SPECT as a tool for characterizing the segmental amyloid burden in ATTR cardiomyopathy. ^{99m}Tc -HMDP SPECT allows to estimate the regional amyloid burden and make some assumptions about disease evolution across Perugini stages.

Myocardial scintigraphy with diphosphonate tracers is a pillar of non-invasive diagnosis of ATTR cardiomyopathy [7], given the high specificity of myocardial diphosphonate uptake [10]. This technique is commonly available (as bone scintigraphy), and its contraindications are basically limited to pregnancy or breastfeeding [11], which are extremely rare among patients undergoing diagnostic workup for cardiac ATTR.

Increasing diphosphonate uptake in the heart is associated with an apparent parallel reduction in bone uptake on planar imaging, which forms the basis of the Perugini score [5]. It has hitherto been assumed that the tracer is avidly and competitively taken up by the heart with reciprocal reduction in bone uptake [12]. In other words, patients scoring 1 on the Perugini scale would have a lower amyloid burden than those scoring 2, who in turn would have less cardiac amyloid than those scoring 3. Interestingly, this hypothesis has never been verified through histopathological studies, and tracer kinetics across Perugini scores has never been specifically investigated. When Perugini grades are assimilated to evolutive disease stages, the results of diphosphonate SPECT allow to make some assumptions about the natural history of ATTR cardiomyopathy, by suggesting that amyloid accumulation progresses from the septum to the inferior region, then involves the lateral, anterior, and apical regions. The late involvement of the apex might account for the relative preservation of contractility of the apex (“apical sparing”), which is highly sensitive and specific for cardiac amyloidosis [13].

Amyloid deposition leads to an expansion of extracellular spaces, manifesting as LGE at CMR [14]. When assimilating again different Perugini score values to evolutive stages of the disease, we noticed that LGE positivity extended from the septal and inferior regions to the other regions, ultimately involving apical segments, with a similar progression than amyloid accumulation on SPECT imaging. Although segmental LGE patterns were not specifically analyzed, LGE was usually subendocardial or transmural, in agreement with the hypothesis of amyloid deposition starting in subendocardial layers (possibly causing the typical global subendocardial LGE), then expanding towards the subepicardial layers.

Very limited evidence exists about diphosphonate SPECT as an imaging tool for ATTR cardiomyopathy. Following 2 small studies that did not perform a quantification of regional tracer uptake [15,16], 2 studies compared SPECT with another imaging modality, while not performing a quantification of segmental tracer uptake. Sperry et al. evaluated ^{99m}Tc -pyrophosphate SPECT versus strain echocardiography in a cohort of 54 patients with ATTR (2 with Perugini score 1) [17]. Contrary to that study, we performed an analysis on 17 segments instead of basal, mid-cavity and apical regions, and we compared amyloid burden by SPECT with another 3-dimensional technique, namely CMR. In a similar study by Pradel et al., findings from ^{99m}Tc -HMDP SPECT and strain echocardiography were compared. No comparison between the different Perugini scores was performed, and no Perugini 1 patients were included [18].

The studies above did not address the added diagnostic value of SPECT to planar scintigraphy. At present, ATTR cardiomyopathy can be diagnosed with no need for endomyocardial biopsy when clinical and imaging findings are compatible with cardiac amyloidosis, no monoclonal protein is found, and planar scintigraphy shows a Perugini grade 2 or 3 uptake [3]. Our data show that an intense myocardial uptake localized to the septum (particularly in the infero-septal segment) can manifest as grade 1 uptake. Therefore, tomographic imaging showing a prominent diphosphonate uptake within the septum or in the infero-septal segment, together with no evidence of monoclonal component, might strengthen the suspicion of ATTR cardiomyopathy. Dedicated studies examining

the diagnostic yield of this approach, and the possibility to avoid the need for histological examination in patients with Perugini score 1 are warranted.

Some limitations of this hypothesis-generating study must be acknowledged. First, 92% of patients scored 2 or 3 on the Perugini scale, reflecting the fact that ATTR cardiomyopathy is usually diagnosed in a relatively advanced stage. Only 8% of patients (n=3) scored 1 on the Perugini scale, although this is the patient subset where SPECT imaging is more likely to show an additive value over planar scintigraphy. Additionally, patients with amyloid light-chain amyloidosis were not evaluated, although they may score 1 on the Perugini scale. Second, segmental and regional ^{99m}Tc -HMDP uptake is likely influenced by wall thickness, which decreases from the basis to the apex. A normalization of tracer uptake by wall thickness was not performed because CZT SPECT did not allow to measure wall thickness, and we preferred not to use values from CMR examinations. Third, the study had a retrospective, cross-sectional design, and relied on the assumption that Perugini score values could be assimilated to different disease stages. Longitudinal studies with serial SPECT examinations would be needed to track disease progression, possibly also in the perspective of stratifying patient risk and assessing the response to therapy. Fourth, the role of SPECT imaging for diagnostic purposes, and possibly for other applications (such as assessment of the response to treatment), remains to be specifically examined. Fifth, this study focused primarily on SPECT imaging, and tissue characterization by CMR was limited to LGE presence or absence in the 17 LV segments. Nonetheless, amyloidosis is a diffuse disease, and T1 mapping techniques such as native T1 and extracellular volume fraction might have been more informative than LGE.

In conclusion, the intensity of segmental uptake of ^{99m}Tc -HMDP SPECT varies across Perugini grades. This allows to hypothesize that amyloid deposition progresses from the septum to the inferior wall and then to the other regions and from the basis to the apex, and also that SPECT imaging might have an additive diagnostic value in patients with very limited uptake in the cardiac region at planar scintigraphy (Perugini score 1).

Figure legends

Figure 1. ^{99m}Tc -hydroxymethylene diphosphonate (HMDP) uptake across Perugini grades: regional analysis.

Colors reflect the intensity of tracer uptake, according to the semiquantitative scale reported in the **Methods** section.

Figure 2. Regional uptake across Perugini scores.

Single photon emission computed tomography (SPECT) results from 3 patients scoring 1, 2, and 3 on the Perugini scale. Amyloid accumulation, manifesting as ^{99m}Tc -hydroxymethylene diphosphonate (HMDP) uptake, starts from the infero-septal region and progressively extends to the whole left ventricle, partially sparing the true apex.

Figure 3. Basal-to-apical ^{99m}Tc -hydroxymethylene diphosphonate (HMDP) uptake across Perugini grades.

Ratios of the average value of ^{99m}Tc -HMDP uptake in basal segments to average value in apical segments were calculated and plotted as a function of Perugini grades.

References

1. Gertz MA, Benson MD, Dyck PJ, Grogan M, Coelho T, Cruz M, Berk JL, Plante-Bordeneuve V, Schmidt HHJ, Merlini G. Diagnosis, prognosis, and therapy of transthyretin amyloidosis. *J Am Coll Cardiol*. 2015;66:2451-66. doi: 10.1016/j.jacc.2015.09.075.
2. Coelho T, Maurer MS, Suhr OB. THAOS: The Transthyretin Amyloidosis Outcomes Survey: initial report on clinical manifestations in patients with hereditary and wild-type transthyretin amyloidosis. *Curr Med Res Opin*. 2013;29:63-76. doi: 10.1185/03007995.2012.754348.
3. Gillmore JD, Maurer MS, Falk RH, Merlini G, Damy T, Dispenzieri A, Wechalekar AD, Berk JL, Quarta CC, Grogan M, Lachmann HJ, Bokhari S, Castano A, Dorbala S, Johnson GB, Glaudemans AW, Rezk T, Fontana M, Palladini G, Milani P, Guidalotti PL, Flatman K, Lane T, Vonberg FW, Whelan CJ, Moon JC, Ruberg FL, Miller EJ, Hutt DF, Hazenberg BP, Rapezzi C, Hawkins PN. Nonbiopsy diagnosis of cardiac transthyretin amyloidosis. *Circulation*. 2016;133:2404-12. doi: 10.1161/CIRCULATIONAHA.116.021612.
4. Glaudemans AW, van Rheenen RW, van den Berg MP, Noordzij W, Koole M, Blokzijl H, Dierckx RA, Slart RH, Hazenberg BP. Bone scintigraphy with (99m)technetium-hydroxymethylene diphosphonate allows early diagnosis of cardiac involvement in patients with transthyretin-derived systemic amyloidosis. *Amyloid*. 2014;21:35-44. doi: 10.3109/13506129.2013.871250.
5. Perugini E, Guidalotti PL, Salvi F, Cooke RM, Pettinato C, Riva L, Leone O, Farsad M, Ciliberti P, Bacchi-Reggiani L, Fallani F, Branzi A, Rapezzi C. Noninvasive etiologic diagnosis of cardiac amyloidosis using 99mTc-3,3-diphosphono-1,2-propanodicarboxylic acid scintigraphy. *J Am Coll Cardiol*. 2005;46:1076-84. doi: 10.1016/j.jacc.2005.05.073.
6. Task Force Members, Montalescot G, Sechtem U, Achenbach S, Andreotti F, Arden C, Budaj A, Bugiardini R, Crea F, Cuisset T, Di Mario C, Ferreira JR, Gersh BJ, Gitt AK, Hulot JS, Marx N, Opie LH, Pfisterer M, Prescott E, Ruschitzka F, Sabaté M, Senior R, Taggart DP, van der Wall EE, Vrints CJ; ESC Committee for Practice Guidelines, Zamorano JL,

- Achenbach S, Baumgartner H, Bax JJ, Bueno H, Dean V, Deaton C, Erol C, Fagard R, Ferrari R, Hasdai D, Hoes AW, Kirchhof P, Knuuti J, Kolh P, Lancellotti P, Linhart A, Nihoyannopoulos P, Piepoli MF, Ponikowski P, Sirnes PA, Tamargo JL, Tendera M, Torbicki A, Wijns W, Windecker S; Document Reviewers, Knuuti J, Valgimigli M, Bueno H, Claeys MJ, Donner-Banzhoff N, Erol C, Frank H, Funck-Brentano C, Gaemperli O, Gonzalez-Juanatey JR, Hamilos M, Hasdai D, Husted S, James SK, Kervinen K, Kolh P, Kristensen SD, Lancellotti P, Maggioni AP, Piepoli MF, Pries AR, Romeo F, Rydén L, Simoons ML, Sirnes PA, Steg PG, Timmis A, Wijns W, Windecker S, Yildirim A, Zamorano JL. 2013 ESC guidelines on the management of stable coronary artery disease: the Task Force on the management of stable coronary artery disease of the European Society of Cardiology. *Eur Heart J*. 2013;34:2949-3003. doi: 10.1093/eurheartj/ehs296.
7. Agostini D, Marie PY, Ben-Haim S, Rouzet F, Songy B, Giordano A, Gimelli A, Hyafil F, Sciagrà R, Bucerius J, Verberne HJ, Slart RH, Lindner O, Übleis C, Hacker M; Cardiovascular Committee of the European Association of Nuclear Medicine (EANM). Performance of cardiac cadmium-zinc-telluride gamma camera imaging in coronary artery disease: a review from the cardiovascular committee of the European Association of Nuclear Medicine (EANM). *Eur J Nucl Med Mol Imaging*. 2016;43:2423-2432. doi: 10.1007/s00259-016-3467-5.
 8. Perugini E, Guidalotti PL, Salvi F, Cooke RM, Pettinato C, Riva L, Leone O, Farsad M, Ciliberti P, Bacchi-Reggiani L, Fallani F, Branzi A, Rapezzi C. Noninvasive etiologic diagnosis of cardiac amyloidosis using ^{99m}Tc-3,3-diphosphono-1,2-propanodicarboxylic acid scintigraphy. *J Am Coll Cardiol*. 2005;46:1076-84. doi: 10.1016/j.jacc.2005.05.073.
 9. Aquaro GD, Camastra G, Monti L, Lombardi M, Pepe A, Castelletti S, Maestrini V, Todiere G, Masci P, di Giovine G, Barison A, Dellegrottaglie S, Perazzolo Marra M, Pontone G, Di Bella G; working group “Applicazioni della Risonanza Magnetica” of the Italian Society of Cardiology. Reference values of cardiac volumes, dimensions, and new functional parameters

- by MR: A multicenter, multivendor study. *J Magn Reson Imaging*. 2017;4:1055-67. doi: 10.1002/jmri.25450.
10. Cappelli F, Gallini C, Di Mario C, Costanzo EN, Vaggelli L, Tutino F, Ciaccio A, Bartolini S, Angelotti P, Frusconi S, Farsetti S, Vergaro G, Giorgetti A, Marzullo P, Genovesi D, Emdin M, Perfetto F. Accuracy of ^{99m}Tc-Hydroxymethylene diphosphonate scintigraphy for diagnosis of transthyretin cardiac amyloidosis. *J Nucl Cardiol*. 2019;26:497-504. doi: 10.1007/s12350-017-0922-z.
 11. Van den Wyngaert T, Strobel K, Kampen WU, Kuwert T, van der Bruggen W, Mohan HK, Gnanasegaran G, Delgado-Bolton R, Weber WA, Beheshti M, Langsteger W, Giammarile F, Mottaghy FM, Paycha F; EANM Bone & Joint Committee and the Oncology Committee. The EANM practice guidelines for bone scintigraphy. *Eur J Nucl Med Mol Imaging*. 2016;43:1723-38. doi: 10.1007/s00259-016-3415-4.
 12. Hutt DF, Quigley AM, Page J, Hall ML, Burniston M, Gopaul D, Lane T, Whelan CJ, Lachmann HJ, Gillmore JD, Hawkins PN, Wechalekar AD. Utility and limitations of 3,3-diphosphono-1,2-propanodicarboxylic acid scintigraphy in systemic amyloidosis. *Eur Heart J Cardiovasc Imaging*. 2014;15:1289-98. doi: 10.1093/ehjci/jeu107.
 13. Phelan D, Collier P, Thavendiranathan P, Popović ZB, Hanna M, Plana JC, Marwick TH, Thomas JD. Relative apical sparing of longitudinal strain using two-dimensional speckle-tracking echocardiography is both sensitive and specific for the diagnosis of cardiac amyloidosis. *Heart*. 2012;98:1442-8. doi: 10.1136/heartjnl-2012-302353.
 14. Perugini E, Rapezzi C, Piva T, Leone O, Bacchi-Reggiani L, Riva L, Salvi F, Lovato L, Branzi A, Fattori R. Non-invasive evaluation of the myocardial substrate of cardiac amyloidosis by gadolinium cardiac magnetic resonance. *Heart*. 2006;92:343-9. doi: 10.1136/hrt.2005.061911.
 15. Minutoli F, Di Bella G, Mazzeo A, Donato R, Russo M, Scribano E, Baldari S. Comparison between (^{99m}Tc)-diphosphonate imaging and MRI with late gadolinium enhancement in

- evaluating cardiac involvement in patients with transthyretin familial amyloid polyneuropathy. *Am J Roentgenol*. 2013;200:W256-65. doi: 10.2214/AJR.12.8737.
16. Fontana M, Pica S, Reant P, Abdel-Gadir A, Treibel TA, Banypersad SM, Maestrini V, Barcella W, Rosmini S, Bulluck H, Sayed RH, Patel K, Mamhood S, Bucciarelli-Ducci C, Whelan CJ, Herrey AS, Lachmann HJ, Wechalekar AD, Manisty CH, Schelbert EB, Kellman P, Gillmore JD, Hawkins PN, Moon JC. Prognostic value of late gadolinium enhancement cardiovascular magnetic resonance in cardiac amyloidosis. *Circulation*. 2015;132:1570-9. doi: 10.1161/CIRCULATIONAHA.115.016567.
17. Sperry BW, Vranian MN, Tower-Rader A, Hachamovitch R, Hanna M, Brunken R, Phelan D, Cerqueira MD, Jaber WA. Regional variation in technetium pyrophosphate uptake in transthyretin cardiac amyloidosis and impact on mortality. *JACC Cardiovasc Imaging*. 2018;11:234-242. doi: 10.1016/j.jcmg.2017.06.020.
18. Pradel S, Brun S, Victor G, Pascal P, Fournier P, Ribes D, Lavie-Badie Y, Galinier M, Carrié D, Berry I, Lairez O; Toulouse Amyloidosis Research Network collaborators. Pattern of myocardial (99m)Tc-HMDP uptake and impact on myocardial function in patients with transthyretin cardiac amyloidosis. *J Nucl Cardiol*. 2018 Jun 7. doi: 10.1007/s12350-018-1316-6. [Epub ahead of print]

Author statement

Chrysanthos Grigoratos: Data curation, Writing- Original draft preparation

Alberto Aimo: Data curation, Writing- Original draft preparation

Claudio Rapezzi: Supervision and Reviewing

Dario Genovesi: Visualization, Investigation, Writing- Reviewing and Editing

Andrea Barison: Visualization, Investigation, Writing- Reviewing and Editing

Giovanni Donato Aquaro: Visualization, Investigation, Writing- Reviewing and Editing

Giuseppe Vergaro: Writing- Reviewing and Editing

Angela Pucci: Visualization, Investigation, Writing- Reviewing and Editing

Claudio Passino: Visualization, Investigation, Writing- Reviewing and Editing

Paolo Marzullo: Visualization, Investigation, Writing- Reviewing and Editing

Alessia Gimelli: Visualization, Investigation, Writing- Reviewing and Editing

Michele Emdin: Writing- Reviewing and Editing

Table 1. Population characteristics.

	Patients n=38	Perugini 1 n=3 (8%)	Perugini 2 n=20 (53%)	Perugini 3 n=15 (40%)	p
Age (years)	81 (76-83)	76 (76-79)	82 (79-83)	81 (80-84)	0.561
Male sex (n, %)	30 (79)	3 (100)	16 (80)	11 (73)	0.578
BMI (kg/m ²)	27.5 (24.3-30.0)	27.9 (26.2-28.7)	26.6 (24.0-29.7)	27.4 (24.9-30.1)	0.731
AF (n, %)	13 (43)	1 (33)	7 (35)	6 (40)	0.754
LBBB (n, %)	3 (11)	0 (0)	0 (0)	2 (13)	0.289
Hemoglobin (g/dL)	12.4 (11.6-13.6)	13.0 (12.7-13.6)	13.1 (11.3-12.9)	12.4 (10.7-13.5)	0.406
eGFR (mL/min)	52 (44-81)	62 (50-73)	48 (34-62)	56 (49-81)	0.050
NT-proBNP (ng/L)	3690 (1493-7420)	2515 (1677-4870)	5491 (3800-8134)	3652 (1827-9426)	0.382
NYHA I/II/III (n, %)	8/14/16 (21/37/42)	1/1/1 (33/33/33)	4/7/9 (20/35/45)	3/6/6 (20/40/40)	0.981
ATTRwt/ATTRv (n, %)	35/3 (92/8)	3/0 (100/0)	18/2 (90/10)	14/1 (93/7)	0.456
Echocardiogram					
IV septal thickness (mm)	19 (16-21)	14 (13-16)	18 (15-20)	21 (19-23)	0.002
PW thickness (mm)	17 (15-18)	12 (12-13)	15 (14-18)	17 (16-19)	0.005
RWT	0.76 (0.62-0.91)	0.45 (0.44-0.51)	0.71 (0.62-0.92)	0.83 (0.75-0.91)	0.008
E/e' ratio	19 (15-20)	17 (15-18)	17 (13-21)	19 (17-21)	0.373

CMR					
LVEDVi (mL/m ²)	81 (64-96)	81 (68-100)	60 (58-96)	82 (68-97)	0.787
LVESVi (mL/m ²)	34 (26-42)	22 (22-42)	26 (23-36)	37 (30-46)	0.515
LVMI (g/m ²)	125 (99-151)	87 (85-96)	109 (94-129)	138 (119-153)	0.054
LVEF (%)	55 (47-65)	73 (61-77)	62 (53-66)	48 (40-62)	0.171
LGE presence (n, %)	38 (100)	3 (100)	20 (100)	15 (100)	-
LA area index (mm/m ²)	17 (15-19)	18 (17-18)	17 (17-20)	16 (14-18)	0.890
RVEDVi (mL/m ²)	74 (65-81)	73 (63-87)	75 (62-83)	80 (71-104)	0.495
RVESVi (mL/m ²)	34 (25-40)	29 (22-41)	32 (24-40)	39 (30-56)	0.629
RVEF (%)	53 (46-63)	51 (49-66)	55 (45-62)	47 (36-54)	0.669
RA area index (mm/m ²)	14 (13-17)	12 (10-16)	13 (13-16)	15 (13-18)	0.397
Pericardial effusion (n, %)	11 (29)	0 (0)	6 (30)	5 (33)	0.498
Pleural effusion (n, %)	14 (37)	1 (33)	6 (30)	7 (47)	0.657

Estimated glomerular filtration rate (eGFR) is calculated through the Chronic Kidney Disease Epidemiology Collaboration (CKD-EPI) equation. AF, atrial fibrillation; ATTRm, mutated transthyretin amyloidosis; ATTRwt, wild-type transthyretin amyloidosis; BMI, body mass index; CMR, cardiac magnetic resonance; ECV, extracellular volume; IV, interventricular; LA, left atrium; LBBB, left bundle branch block; LGE, late gadolinium enhancement; LVEDVi, left ventricular end-diastolic volume index; LVESVi, left ventricular end-systolic volume index; LVEF, left ventricular ejection fraction; LVMI, left ventricular mass index; MI, myocardial infarction; NT-proBNP, N-terminal fraction of pro-brain natriuretic peptide; PW, posterior wall; RA, right atrium; RVEDVi, right ventricular end-diastolic volume; RVEF, right ventricular ejection fraction; RVEDVi, right ventricular end-systolic volume index; RWT, relative wall thickness.

Journal Pre-proof

Highlights

- In ATTR cardiomyopathy, SPECT allows to characterize regional amyloid burden.
- SPECT also allows to quantify the intensity of amyloid burden.
- Amyloid deposition begins in the septal and inferior walls and the basal region.